Comparison of Coupling Mechanisms on Multiconductor Cables

Frédéric Broydé, *Member, IEEE*, and Evelyne Clavelier, *Member, IEEE*

Abstract— **Five possible types of coupling on multiconductor cables are identified. The three new types of coupling have their respective magnitudes assessed, for different simple cables. We then give a complete example of field-to-cable coupling calculation with the five types of coupling included. An experiment reproducing the setup considered in this calculation was carried out and shows that one of the coupling described by the parallel transfer impedance (coupling type 3) is present and dominates the cable response in certain cases.**

I. Introduction

FOLLOWING early work by Schelkunoff in the 1930's, the effort concerning the modeling and measurement of the shielding characteristics of coaxial cables has been tremendous in the past 25 years. It is now well established that, up to 3 GHz, a coaxial cable is best characterized by a transfer impedance and a through elastance [1]. Above that frequency limit, these two quantities may still be relevant, but are more difficult to measure, and shielding effectiveness is still used for the characterization of coaxial cables. As we will use transfer impedance and through elastance, one may consider that our paper is restricted to frequencies below 3 GHz, but some considerations which we will develop are not frequency-dependant.

Throughout this paper, we will only study shielded multiconductor cables with one or more internal wires and one overall shield. The paper is also limited to cables of circular (or approximately circular) cross section. Our ideas could of course easily be extended to more complex cables. Several authors have already developed concepts and measurement techniques for shielded multiconductor cables. In some cases, the concepts of common-mode and differential-mode transfer impedance have been introduced and those quantities directly measured [2]. However, those quantities could theoretically be deduced from the knowledge of the complex transfer impedance for each wire contained in the shield. Though the direct measurements of common-mode and differential-mode transfer impedance have a practical interest, they do not describe other coupling phenomena than those used for coaxial cables.

The purpose of this paper is to show that other coupling mechanisms indeed exist in multiconductor shielded cables, to suggest measurement techniques, and to evaluate them.

Manuscript received September 1, 1992; revised May 6, 1993. This work was supported by the Etablissement Technique Central de l'Armement (ETCA), Arcueil, France.

The authors are with EXCEM, 12, Chemin des Hauts de Clairefontaine, 78580 Maule, France.

IEEE Log Number 9211298.

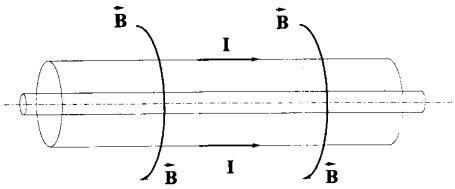

Fig. 1. Type 1 coupling on a coaxial cable.

Throughout the paper something "having a cylindrical symmetry" means that it is invariant by any orthogonal transformation that leaves a cylinder of circular cross section invariant. Let us recall that these include translation along the axis, rotation around the axis, symmetry with respect to any plane that contains the axis, or orthogonal to the axis. At any given point, the words axial, radial, and orthoradial, respectively, mean "parallel to the cable axis," "orthogonal to the axis and along a straight line crossing the axis," and "orthogonal to any axial vector and to any radial vector."

II. Cables with Cylindrical Symmetry

Let us consider a cable with a single shield, characterized by a perfect cylindrical symetry, but having possibly all and any limitations normally found on real cables: diffusion coupling, aperture coupling, porpoising coupling, etc. First of all, this cable can only be a coaxial cable. What could we say of the shielding properties of this coaxial cable, if we knew nothing of the existing theory?

To begin with, we could find that the possible causes of coupling through the shield would be electric field (possibly caused by charges far away from the cable), magnetic field (possibly caused by currents far away from the cable), currents on the cable, and charges on the cable. We would then try different field configurations and find out that because of the cylindrical symmetry of the coaxial cable, there is only four situations of interest, respectively, one for the electric field, one for the magnetic field, one for charges, and one for currents. Applying basic electromagnetic laws would then force us to merge those four situations into two types of coupling.

Fig. 1 shows what we call type 1 coupling on a coaxial cable: a common-mode current flows on the screen and an orthoradial magnetic field surrounds the cable. As we know, the cable is completely characterized for this coupling by its (linear) transfer impedance Z_T (in ohms per meter) which relates the inner voltage per unit length to the common-mode current.

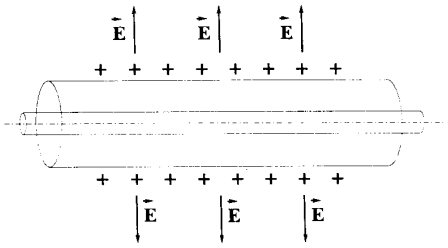

Fig. 2. Type 2 coupling on a coaxial cable.

Fig. 2 shows what we call type 2 coupling on a coaxial cable: charges appear on the surface of the cable and a radial electric field surrounds the cable. As we know, the behavior of the cable for this coupling may be characterized by a through elastance or a transfer admittance. As the latter is not a characteristic of the cable only, one usually voids its use for cable characterization. Let us recall [1] that in a triaxial measurement setup, the transfer admittance Y_T is related to the through elastance K_T by

$$K_T = \frac{Y_T}{j\omega C_1 C_2} \tag{1}$$

where C_1 is the per-unit-length capacitance of the outer circuit and C_2 is the per-unit-length capacitance between the two conductors of the coaxial cable. The through elastance is a characteristic of the cable only, and Y_T is dependant on the measurement setup because C_1 will differ from one test-installation to the other, if their transverse dimensions are different. However, we prefer to introduce a new quantity ζ_R called the radial electric coupling coefficient. The radial electric coupling coefficient is dimensionless, and defined as

$$\zeta_R = \frac{Y_T}{j\omega C_1}. \tag{2}$$

It has the advantage of being a quantity depending on the cable only, and also to have a clear physical significance: it may be interpreted as the ratio of the per-unit-length current injected into the inner conductor on the per-unit-length displacement current impinging on the shield.

Let us note that pure type 1 and pure type 2 coupling are only possible on a length of cable short compared with wavelength, because current may not propagate without charges accumulating somewhere, and because charges need to be brought from somewhere by a current. This does not contradict the independance of the two coupling types.

III. Cable with Good Shield Having Cylindrical Symmetry

Let us follow the same approach as previously for a multiconductor shielded cable, which may contain any strictly positive integer number n of internal wires (coaxial cables are included), with the two following assumptions:

- the shield has a perfect cylindrical symmetry,
- the shield is good: by this we mean that it offers enough screening for the weak coupling approximation to be valid.

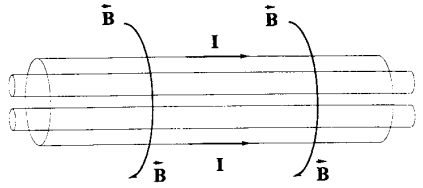

Fig. 3. Type 1 coupling on a shielded multiconductor cable.

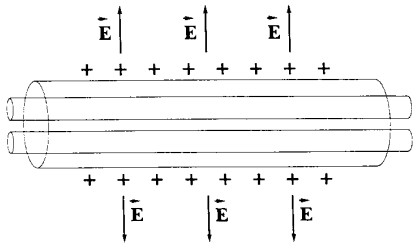

Fig. 4. Type 2 coupling on a shielded multiconductor cable.

Under the weak coupling approximation, a stimulus on one side (side 1) of the shield may have effects on current and charges on the other side (side 2) of the screen, but these effects have negligible consequences on charges and current on the side (side 1) where the stimulus takes place. Therefore, even though the cable as a whole does not have the cylindrical symmetry, in the case of a external excitation the current on the screen establish themselves as if the cylindrical symmetry was present.

With these two hypotheses, we now find five different types of coupling. These couplings will be explained with figures which represent a shielded pair, having three obvious planes of symmetry. This representation was used for the clarity of our drawings, but the cable considered may have any number of internal wires, and no symmetry is assumed, though it may eventually be present.

Fig. 3 illustrates type 1 coupling. It is similar to the type 1 coupling for shielded cables. The characteristics of the cable for this coupling may be expressed for this coupling with n complex transfer impedances (one for each internal wire), as said in the introduction. We wrote explicitly that we consider the complex quantity, because we want to outline that the phase relationship between the voltage induced on the different conductors is extremely important. For instance, in the case $n = 2$, two voltages in phase are in common mode, and two signals with opposite phase are in differential mode: their possible effects on a susceptible device are different as well as the applicable mitigation practices.

Fig. 4 illustrates type 2 coupling. It is also similar to type 2 coupling for shielded cables. The cable could be characterized for this type of coupling with n complex transfer admittances, but these transfer admittances are not a property of the cable only, as in the case of the coaxial cable. The simplest solution to characterize the cable for type 2 coupling is to use n complex radial electric coupling coefficients, which are obviously a property of the cable only.

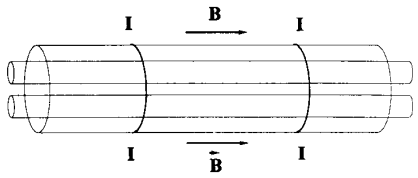

Fig. 5. Type 3 coupling on a shielded multiconductor cable.

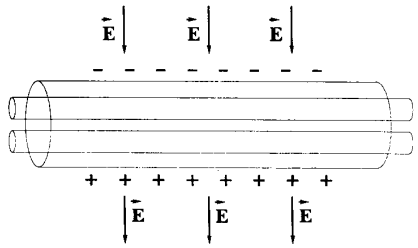

Fig. 6. Type 4 coupling on a shielded multiconductor cable.

Fig. 5 illustrates type 3 coupling. Here the current is orthoradial, and the magnetic field is axial. This is typically what would have been observed if the cable were placed on the axis of a coil. Coupling with the internal wires will not occur if those cables are straight. However, a voltage will clearly be induced on skewed wires, an example of which is the twisted pair. It does not seem natural to relate the induced voltage to the current. We prefer to introduce a quantity that would relate the voltage per unit length on a given wire to the axial magnetic field $\boldsymbol{H}$ (in amperes per meter). We shall call this quantity the axial transfer impedance (in ohms), and we need n axial transfer impedances to characterize the cable with respect to type 3 coupling.

Fig. 6 illustrates type 4 coupling. A parallel electric field orthogonal to the axis is present. Its orientation is such around the cable that it produces no net charge per unit length of cable. This is what would happen if the cable is introduced at the center of two parallel plates excited by a symmetrical voltage source. As an example, if one considers the configuration shown on Fig. 6 and if we assume a perfect symmetry with charge reversal, with respect to the plane between the two internal wires, a pure differential mode current is induced on the two wires (we also assume symmetrical terminations at both ends); this is totally different from type 2 coupling which, with the same assumptions, would bring a pure common mode current on the two wires. It sounds logical to describe this coupling with a quantity that relates the per-unit-length current received on a wire to the per-unit-length displacement current that flows into the cable on one side and leaves it on the other. We call this quantity the parallel electric coupling coefficient. As usual we need n such complex quantities to characterize the cable with respect to type 4 coupling, but it must be outlined that these are *a priori* dependant on the orientation of the electric field.

Fig. 7 illustrates type 5 coupling. A magnetic field passes through the cable, penetrates the shield and directly induces

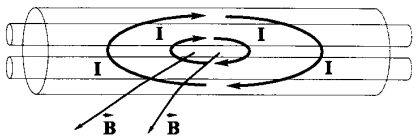

Fig. 7. Type 5 coupling on a shielded multiconductor cable.

voltages between the cable's conductors. Unlike the other types of coupling until now, this coupling places the magnetic field in a "forbidden" orientation: the laws of electromagnetics say that magnetic fields must run parallel to good conductors. In fact this should not disturb us to much because we are obviously dealing with imperfect shields, made of imperfect conductors. This type of coupling could be produced if we install the cable inside an Helmholtz coil, orthogonal to its axis. We propose to describe this phenomenon with a quantity defined for each inner wire as the ratio between the per-unit-length voltage induced with respect to cable shield, to the amplitude of the impinging magnetic field (in amperes per meter). We call this quantity the parallel transfer impedance of the cable (in ohms). As previously, we need n complex parallel transfer impedances, which are *a priori* dependant on the orientation of the magnetic field.

Let us conclude this section with three remarks.

1) From the above definitions it is clear that for a coaxial cable as defined in Section II, the axial transfer impedance, the parallel electric coupling coefficient and the parallel transfer impedance all vanish. This would not necessarily be true for an imperfect coaxial cable.
2) As was said for cable with cylindrical symmetry, for any integer x between 1 and 5, pure type x coupling is only possible for an electrically short length of cable.
3) We introduced five types of coupling, but we could have introduced more of them! In fact the action of a general electromagnetic field on a cable can be expanded in an infinite series of terms having increasingly more complex symmetry. Appendix I gives an example of such a series (for electric-field excitation), and shows that the first two terms are associated with coupling types 2 and 4. We limited ourselves with five types of coupling because we believed that these types could account for most situations of interest.

IV. Real Cables of Circular Cross Section

This section deals with the definition of the coupling types for a cable of circular or almost circular cross section, without assumption of cylindrical symmetry. Obviously, for such a cable, we can nevertheless keep the idea of defining five coupling modes, provided we define them according to the symmetry of the incident field, as it appears in the definition given previously.

Let us, for instance, consider a simple coaxial cable with a tape-wound screen. The shield does not have the cylindrical symmetry, though it is of circular or almost circular cross section. This type of cable does not belong to the categories of cable discussed in the Sections II and III above. For instance, if such a cable is excited by an orthoradial magnetic field, we

will call this a type 1 coupling, but the current on the screen will usually (especially at low frequencies, see [4]) flow in an helicoidal path, instead of flowing along the cable axis. Also, the total magnetic field along the cable will no longer be orthoradial, because of the field produced by the skewed currents on the screen.

We must, therefore, be very careful that (because we define the types of coupling according to the symmetries of the incident field) the properties of the charge and current distributions mentioned in Section III are not necessarily present. This will be shown experimentally in Section VIII.

Up to now, the paper has been mainly based on considerations of symmetry. The purpose was to identify different possible types of coupling. The problem of the mechanisms of a possible coupling has not yet been addressed. This will be the subject of the next sections.

V. Evaluation of Coupling Magnitudes

Our purpose in this section is to calculate the new coupling parameters in the most simple cases, in order to justify and illustrate the five types of coupling concept. Coupling types 1 and 2 being well understood, we will review in some detail types 3, 4, and 5 coupling. Everything in this section is limited to frequencies when the cable radius is much smaller than the wavelength.

For type 3 coupling, we can easily compute the axial transfer impedance in the case of an homogeneous cylindrical shield of circular cross section, of radius r_0 and thickness d. Kaden (see [3, p. 78, eq. (21)]) already did most of the work when he found that in this field configuration the internal field is uniform, and computed the shielding factor as

$$Q_3 = \frac{1}{\cosh\left(\frac{1+j}{\delta}d\right) + \frac{1}{2}K\sinh\left(\frac{1+j}{\delta}d\right)} \tag{3}$$

where

$$K = \frac{\mu_O}{\mu}\frac{1+j}{\delta}r_O \tag{4}$$

δ being the skin depth at the given frequency. Obviously, the axial transfer impedance vanishes for straight wires. Let us, therefore, consider that the cable contains twisted wires, the wire i being wound at m_i turns per meter, on an helix of radius r_i. If left unconnected, the wires inside the shield (these wires are supposed to be of a nonmagnetic material) do not disturb the magnetic field; if one or more wires are connected, their interaction with the magnetic field may be taken care of by the proper use of the inductance matrix. The axial-transfer impedance $Z_{\mathrm{AT}i}$ for wire i is therefore given by

$$Z_{\mathrm{AT}i} = \frac{j\omega\mu_o m_i \pi r_i^2}{\cosh\left(\frac{1+j}{\delta}d\right) + \frac{1}{2}K\sinh\left(\frac{1+j}{\delta}d\right)}. \tag{5}$$

By analogy with the theory of transfer impedance (type 1 coupling), these formulas describe the diffusion coupling. Of course, of more practical interest would be the case of aperture coupling (or of other phenomena), but we did not try to compute it. It should be noted that the authors initially believed that for a shielded twisted pair, m took two values of opposite signs. This is not correct, and the values are instead almost equal, giving predominantly rise to common-mode coupling.

Let us now have a look at type 4 coupling. From electric-field shielding theory we know that for a homogeneous shield, the parallel electric coupling coefficient will be zero or extremely small (the same is true for the radial electric coupling coefficient). The cable shields that suffer from a significant type 2 or type 4 couplings need to have apertures, they do not have the cylindrical symmetry, and the cables fall into the category discussed in Section IV. Let us therefore consider a two-wire cable with apertures in its shield, having equal radial electric coupling coefficients ζ_{R1} and ζ_{R2} for wires 1 and 2. In the very special case for which we assume that the shield has perfect cylindrical symmetry, we can assess an order of magnitude for the parallel electric coupling coefficients ζ_{P1} and ζ_{P2} for wires 1 and 2. To achieve this, we will consider a shielded pair containing two straight wires. The external problem is easy to solve, and one finds that the surface charge density on the outer surface of the shield is

$$\rho_S = 2\varepsilon_o E\cos\theta \tag{6}$$

where E is the intensity of the incident electric field, and θ is the angle of cylindrical coordinates. The internal problem is much more difficult. For the worst orientation, one may assume that all positive (respectively, negative) charges have field lines that fall on wire 1 (respectively, wire 2). In that case, it sounds reasonable to assume that

$$\zeta_{P1} \approx \zeta_{R1} \tag{7}$$

$$\zeta_{P2} \approx \zeta_{R2} \tag{8}$$

gives at least an adequate order of magnitude for the parallel electric coupling coefficients. It seems to us that a more serious theoretical investigation of this coupling requires numerical solution of the field internal to the shield. Also let us recall that Vance [4] gives estimate of the through elastance for single-braid shields. The value he finds for cables like RG58 is about 3×10^7 m/F. This is equivalent to a radial electric coupling coefficient ζ_R of about 3×10^{-3}. For a cable having an RG58-like shield containing two wires, a reasonable estimate of the radial electric coupling coefficient for one wire would be the half of this value. Finally, let us observe that twisting internal wires is a mean of reducing the parallel electric coupling coefficient.

Let us now consider type 5 coupling. In this case we need to evaluate, for each wire, the voltage induced in the wire-shield loop. The computation is generally not easy, and we will only consider the case of a cable having two wires, and three orthogonal planes of symmetry. In this case, one only needs to compute the voltage induced in the wire 1–wire 2 loop. For a homogeneous cylindrical shield of circular cross section, Kaden (see [3, p. 80, eq. (33)]) again found that in this field configuration, the internal field is homogeneous, the shielding factor being given by

$$Q_5 = \frac{1}{\cosh\left(\frac{1+j}{\delta}d\right) + \frac{1}{2}\left(K + \frac{1}{K}\right)\sinh\left(\frac{1+j}{\delta}d\right)} \tag{9}$$

where the previous definition of d, δ, and K are still valid. Assuming a distance Δ between the two wires, the parallel transfer impedance Z_{PT1} for wire 1 and the parallel transfer impedance Z_{PT2} for wire 2 are given by

$$Z_{PT1} = \frac{\frac{1}{2}j\omega\mu_o\Delta}{\cosh\left(\frac{1+j}{\delta}d\right) + \frac{1}{2}\left(K + \frac{1}{K}\right)\sinh\left(\frac{1+j}{\delta}d\right)} \quad (10)$$

$$Z_{PT2} = \frac{-\frac{1}{2}j\omega\mu_o\Delta}{\cosh\left(\frac{1+j}{\delta}d\right) + \frac{1}{2}\left(K + \frac{1}{K}\right)\sinh\left(\frac{1+j}{\delta}d\right)}. \quad (11)$$

As for the axial transfer impedance (11) and (12) only account for diffusion coupling, and more work is needed to assess aperture coupling or other mechanisms.

VI. Comparison of Coupling Magnitudes

Let us consider a cable having a good shield with cylindrical symmetry. The results of (5), (10), and (11) may easily be compared with the traditional Schelkunoff [4] formula for diffusion coupling. If R_{dc} is the dc per-unit-length resistance of the cable shield, for any internal conductor we have

$$\lim_{\omega\to 0} Z_T = R_{dc} \quad (12)$$

whereas for type 3 coupling and type 5 coupling we have

$$\lim_{\omega\to 0} Z_{AT} = 0 \quad (13)$$

$$\lim_{\omega\to 0} Z_{PT} = 0. \quad (14)$$

For frequencies high enough for the skin depth δ to be much smaller than the shield thickness, one can easily show that

$$\frac{Z_{AT}}{Z_T} \approx 4\pi^2 m_i r_i^2 \quad (15)$$

and

$$\frac{Z_{PT}}{Z_T} \approx 2\pi\Delta. \quad (16)$$

Let us stress that these formulas only account for diffusion coupling, and that they are based on the internal wire geometry and other assumptions for which (5), (10), and (11) have, respectively, been derived.

VII. Calculation of Field-to-Cable Coupling

In this paragraph we give two examples of field-to-cable coupling problems, with a complete expression of the voltage on an internal wire. The calculations are valid for any cable of circular or almost circular cross section, but assume a length of cable electrically short. We have also neglected crosstalk between internal wires, the influence of which would be negligible with our assumptions.

We will first consider the case of a cable the shield of which is in contact with a metallic plane. A plane wave propagates along the cable. This situation is typically what would be obtained if a cable is installed in a rectangular TEM cell, as shown on Fig. 8.

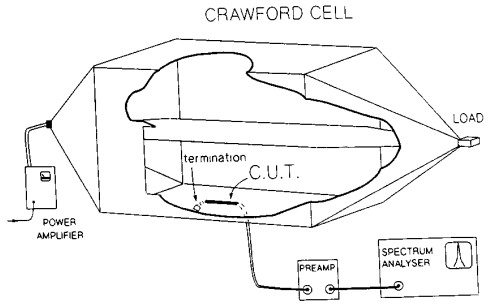

Fig. 8. The longitudinal installation of a CUT (cable under test) inside a TEM cell.

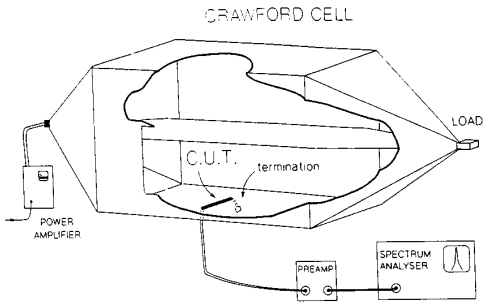

Fig. 9. The transverse installation of a CUT (cable under test) in a TEM cell.

Appendix I shows how the effect of the electric field can be taken care of for a short length of cable. If we now assume that ζ_R and ζ_P have a constant value along the length of cable illuminated by the field, we can say that the electric field causes on a wire i an injection of current equal to

$$I_d \approx \int_0^l 2j\omega r_o\varepsilon_o E\{\zeta_{Pi} - \pi\zeta_{Ri}\}dx = 2j\omega r_o\varepsilon_o El\{\zeta_{Pi} - \pi\zeta_{Ri}\}. \quad (17)$$

Appendix II gives the value of the current along the cable shield. If the length of cable is terminated by an impedance Z_o at both ends, and if η_o is the free-space wave impedance, the voltage ν_i obtained at one termination is given by

$$\frac{\nu_i}{l} \approx \pm\frac{E}{2\eta_o}\{Z_{PTi} + 2\pi r_o Z_{Ti}\} + \frac{j\omega\varepsilon_o E}{Z_o} r_o\{\zeta_{Pi} - \pi\zeta_{Ri}\} \quad (18)$$

where the + sign applies to near-end coupling and the − sign to far-end coupling. For deriving the second term in (18), we have used the total longitudinal current flowing on the cable, and multiplied it by Z_T, even though the current and the magnetic field do not have the symmetry of type 1 coupling. This is justified by the fact that experience like the one carried out in wire-injection [5] measurement, proves that in many cases there is little difference between a measurement

TABLE I
EXPERIMENTAL RESULTS FOR THE FIRST CABLE

Frequency	Measured ν_i/l for $E = 1$ V/m Setup of Fig. 8	Measured ν_i/l for $E = 1$ V/m Setup of Fig. 9
1 MHz	-12.8 dB (μV)	-26.5 dB (μV)
10 MHz	-0.6 dB (μV)	-10.5 dB (μV)

with, and a measurement without a radially inhomogenous longitudinal current.

Let us now consider the case of a cable the shield of which is in contact with a metallic plane, but installed for the broadside incidence of a plane wave propagating along the plane. Once again, this situation may be obtained in a rectangular TEM cell, as shown on Fig. 9. The value ν_i of the voltage at both terminations is now given by

$$\frac{\nu_i}{l} \approx \pm\frac{E}{2\eta_o} Z_{\mathrm{AT}i} + \frac{j\omega\varepsilon_o E}{Z_o} r_o\{\zeta_{Pi} - \pi\zeta_{Ri}\} \qquad (19)$$

where the sign of the first term depends on the termination considered and the convention for the sign of the parameter m_i.

This last expression is of great interest because type 3 coupling is the only term that is independant of the electric field on the cable.

VIII. EXPERIMENTAL RESULTS

The experiments suggested in the previous section (i.e., according to Figs. 8 and 9) have been carried out in the SIEM1 simulator at ETCA, Arcueil, France. The height of the sceptum is 1 m, and the cell width is 2.25 m. For all our measurements, the field strength ranged between 100 and 160 V/m. We checked for all measurements that noise and unwanted coupling were below 30 dB of the measured value. The cable tested were terminated by a 50 Ω resistor at one end, and by the 50 Ω input of our Sonoma Instrument 310 preamplifier at the other end. When the setup of Fig. 8 was used, we measured the far-end coupling.

For the measurements presented in this paper, we wanted to be absolutely certain that no unexpected coupling would occur: we therefore choose not to use a network analyzer or a tracking generator. We made measurements at few discrete frequencies. We show our results at 1 MHz and 10 MHz, frequencies at which the fields inside this TEM cell are "very clean." For both geometries, the cable was centered with respect to the cell's vertical plane of symmetry, in order to counteract imperfection in the field distribution.

The first cable tested had 19 internal wires twisted at 1 turn every 9 cm, a single tinplated cupper braid, and the external diameter of the braid was about 8.5 mm. We chose a wire that was near the braid. The length of cable exposed to the field was 0.5 m. Our results for this cable are shown in Table I, normalized for 1 m of cable and 1 V/m.

It is interesting to notice that the measured value in the transverse position (i.e., according to Fig. 9) is only about 10 dB lower than for the cable in the longitudinal position (i.e., according to Fig. 8). We then wondered if the signal obtained in the transverse position resulted more from magnetic or electric coupling. We therefore installed a plate 70 cm long and 15 cm wide at a height of 6.5 cm above the 50 cm long part of the cable exposed to the field. We then made the same measurement 1) with the plate floating, and 2) with the plate grounded with a 2.5 cm wide strap. In both cases, the reading did not change by more than 1.5 dB (within our estimated measurement errors). However, measurements made with a D-dot sensor proved that our electric screen 1) did not affect the electric field seen by the cable of more than 1 dB when left floating, and 2) did reduce the electric field of 41 dB at 1 MHz and 35 dB at 10 MHz when grounded.

We therefore proved the existence of type 3 coupling with this simple experiment. Assuming that (19) is applicable, the measured value for the axial transfer impedance Z_{AT} are: -89.0 dB (Ω) at 1 MHz and -73 dB (Ω) at 10 MHz.

We also tested the same piece of cable in a conventional triaxial test fixture and we measured the transfer impedance. We obtained -41.8 dB (Ω/m) at 1 MHz and -31.4 dB (Ω/m) at 10 MHz. If we apply (18) to the values in Table I, and neglect Z_{PT} and the electric field coupling terms, we find -43.8 dB (Ω/m) at 1 MHz and -31.6 dB (Ω/m) at 10 MHz. The differences between both sets of values is within 2 dB and is too low to be very significant. It may contain various measurement inaccuracies, nonperfect radial symmetries of the cable assumed in (18), or a significant contribution of Z_{PT}.

The second cable tested was a type KX15, similar to RG58C/U. Our requirement of having a signal 30 dB above noise and unwanted coupling was far from being met at 10 MHz, and the result will therefore not be given. At 1 MHz, we measured $Z_{\mathrm{AT}} = -93.2$ dB (Ω). This high value was totally unexpected, and we checked as previously that our reading was not due to electric field. This proves that a braided shield coaxial cable should not *a priori* be considered as having a cylindrical symmetry (if it had this symmetry, type 3 coupling would not be present).

It is important to add that for all our measurements, the cable was in galvanic contact with the ground plane. However, we also made measurements with the cables a few millimeters above the ground plane surface (but the shield was always grounded at both ends), without any noticeable change in the measured voltages. In fact, the measurements were not really affected by small cable moves. For instance, this precludes that any significant current had flown sideways, with a component on the cable shield, during transverse measurements.

IX. CONCLUSION

This paper presented the concept of five different types of coupling on multiconductor shielded cable of circular or almost circular cross section. We showed that for simple cable structure, the relevant parameters for these types of coupling could be assessed. We also showed how to use the five types of coupling in a field-to-wire coupling problems.

Preliminary experiments prove that type 3 coupling, up to now forgotten in most field-to-cable coupling calculations, cannot be neglected because it gives rise to a cable response in places where the incident magnetic field is parallel to the cable.

Concerning the theory of the mechanisms of the different types of coupling, we are aware that we did the easiest part, leaving computational difficulties to others. We are currently planning to get more experimental data on the new types of coupling (types 3, 4, and 5), as well as on type 2 (we are not aware of any published results for through elastance).

One of the interesting point in this experimental work will be to devise the experiments in such a way that for each of them one type of coupling clearly dominates.

APPENDIX I
CHARGE DISTRIBUTION AND EFFECT OF E FIELD

Fig. 10(a) shows how the electric field lines around the cable look like, this applies to both geometries of Figs. 8 and 9. How shall we compute the charge distribution and the effect of electric field?

First of all we know that the radial distribution of the surface charge density ρ_S can be developed into a Fourier series as

$$\rho_S(\theta) = \rho_{S0} + \rho_{S1}\cos(\theta + \varphi_1) + \rho_{S2}\cos(2\theta + \varphi_2) + \cdots + \rho_{Sn}\cos(n\theta + \varphi_n) + \cdots. \quad (20)$$

The first term in this development, taken alone, would describe the homogeneous charge distribution on a cable isolated in space, as shown in Fig. 10(b). One can easily check that the second term describes the charge distribution of the cable if it were floating in the middle of the two parallel plates of a (large) capacitor, as shown on Fig. 10(b). None of the three parts of Fig. 10 are derived from a calculation, they are only estimates, drawn by hand. However, it seems reasonable that the two first terms in (20) will give an acceptable description of Fig. 10(a). Assuming that we now use this approximation, and taking $\theta = 0$ at the point of contact between the cable and the ground plane, because of the symmetries, and because the surface charge density vanishes at $\theta = 0$, ρ_S becomes

$$\rho_S(\theta) \approx k\varepsilon_o E(\cos\theta - 1) \quad (21)$$

where k is a dimensionless coefficient, and E is the applied (i.e., incident) electric field. The first way of assessing k is to say that if we assume that (21) is exact, we can simply use an analytical approach with the following steps. One must first remove the ground plane, by using the image theorem. The problem to solve now consists of two cables with opposite surface charge distributions. We now apply the superposition theorem to the charge distribution on one cable, as described by (21); the field (infinitely) far from the cable is only related to the term of $\cos\theta$, and (6) gives the field value: 1 V/m at infinity produces a charge distribution of $2\varepsilon_o\cos\theta$ on one cable. If one considers the two cables and their respective charge distributions, this electric field value is doubled: 2 V/m produce a charge distribution of $2\varepsilon_o\cos\theta$ on each cable. Therefore, the value of k is 1.

The second way (harder) is not to trust analytical calculation and to try a numerical approach. We did so with our ICAP/4 simulation software. Fig. 11 shows the equivalent resistor network that we used. All resistors are equal except those at the left and right border and around the cable. We "measure" the total current collected by the cable, equivalent to the total charge. In order to get with (21) the result of our numerical simulation, k would have to take the value 1.07, close enough from the analytical result.

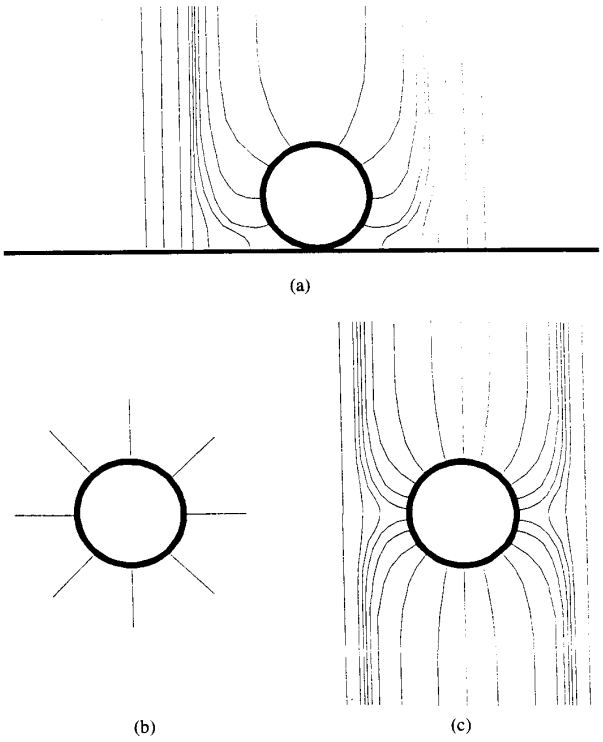

Fig. 10. Shape of the electric field around a cable. (a) Cable inside the cell. (b) Charged cable in free space. (c) Cable between capacitor plates.

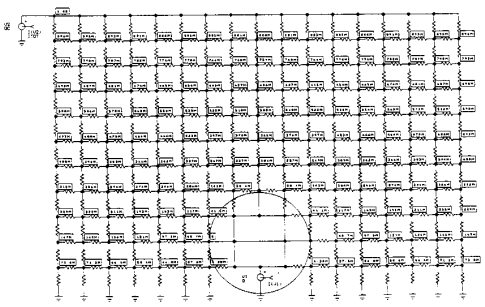

Fig. 11. Schematic used for the calculation of the displacement current on the cable inside the cell, with the ICAP/4 SPICE simulation package. The circle indicates the cable position. The potentials appear inside rectangles.

In the following, we will use $k = 1$, and the surface charge density becomes

$$\rho_S(\theta) \approx \varepsilon_o E(\cos\theta - 1) \quad (22)$$

Anywhere on the ground plane, far from the cable, the surface charge density is only $\varepsilon_o E$. If one integrates (22) on the cable circumference we see that the cable collects the displacement current on a width of $2\pi r_o$. From the definitions of ζ_R and ζ_P, we can compute the displacement current di_d received by

a length dx of cable as

$$\frac{di_d}{dx} \approx j\omega r_o \left\{ 2\pi\zeta_R \rho_{S0} + \zeta_P \int_{-\frac{\pi}{2}}^{\frac{\pi}{2}} \rho_{S1} \cos\theta \, d\theta \right\} \tag{23}$$

which gives

$$\frac{di_d}{dx} \approx 2j\omega r_o \varepsilon_o E\{\zeta_P - \pi\zeta_R\}. \tag{24}$$

APPENDIX II
CURRENT DISTRIBUTION AND TOTAL CURRENT

How can we compute the current flowing along the cable when the cable is installed according to Fig. 8? We will use a property that is only valid at frequencies for which the current may be regarded as a surface distribution, because of the skin effect. At such frequencies, the charge and current distribution inside a transmission line are the same, except for a multiplying constant. Using (22) we get

$$j_S = \frac{E}{\eta_o}(1 - \cos\theta) \tag{25}$$

and the total current flowing on the cable is then

$$I_t = \int_0^{2\pi} \frac{E}{\eta_o}(1 - \cos\theta) r_o \, d\theta \tag{26}$$

$$I_t = 2\pi r_o \frac{E}{\eta_o}. \tag{27}$$

Typically, the skin effect becomes visible on braided cables from 1 MHz. We may assume that the use of (27) will be acceptable at this frequency and above.

ACKNOWLEDGMENT

The authors wish to thank J.-P. Caillou of the Etablissement Technique Central de l'Armement for encouragement and for sponsoring this work. The authors would also like to acknowledge the contribution of P. Vallet to the experimental work presented here, and are grateful for the reviewer comments, which helped improve the paper.

REFERENCES

[1] E. P. Fowler, and L. K. Halme, "State of the art in cable screening measurements," in *Proc. 9th Int. Zürich Symp. EMC*, Mar. 1991, pp. 151–158.
[2] P. Degauque and J. Hamelin, *Compatibilité Électromagnétique*. Paris, France: Dunod, 1990.
[3] H. Kaden, *Wirbelströme und Schirmung in der Nachrichtentechnik*. New York: Springer-Verlag, 1959.
[4] E. F. Vance, *Coupling to Shielded Cables*. New York: Krieger, 1987.
[5] L. Halme and B. Szentkuti, "The background for electromagnetic screening measurements of cylindrical screens," *Bull. Tech. PTT*, no. 3, PTT Suisses, Berne, Switzerland, 1988.

Frédéric Broydé (S'84–M'85) was born in Savigny sur Orge, France, in 1960. He received the "Ingénieur" degree from the Ecole Nationale Supérieure de Physique de Grenoble, Grenoble, France, in 1984.

He co-founded the EXCEM S.A. corporation in May 1988, and became its Chairman. The company is now based in Maule, France, and he manages research or development projects mostly related to EMC. Currently, he works on the hardware of a new type of equipment for the measurement of the shielding effectiveness of enclosure, on the measurement of the shielding properties of cables, on new solid-state active surge protections, and other topics.

Mr. Broydé is a member of the IEEE Electromagnetic Compatibility Society.

Evelyne Clavelier (S'84–M'84) was born in Levallois-Perret, France, in 1961. She received the "Ingénieur" degree from the Ecole Nationale Supérieure de Physique de Grenoble, Grenoble, France, in 1984.

She is co-founder of the EXCEM S.A. Corporation (May 1988) and has become the General Manager of this company. She takes care of supervising scientific calculations and simulations, often related to EMC. Her current fields of interests include the simulation of fast-surge arrestors, and the creation of software of a system for accurate location of defects on undersea cables.